

CESCProg: A compact prognostic model and nomogram for cervical cancer based on miRNA biomarkers

Sangeetha Muthamilselvan¹, Ashok Palaniappan^{Corresp. 1}

¹ Department of Bioinformatics, School of Chemical and Biotechnology, SASTRA Deemed University, Thanjavur, Tamil Nadu 613401, India

Corresponding Author: Ashok Palaniappan
Email address: apalania@sabt.sastra.edu

Cervical squamous cell carcinoma, more commonly cervical cancer, is the fourth common cancer among women worldwide with substantial burden of disease, and less-invasive, reliable and effective methods for its prognosis are necessary today. Micro-RNAs are increasingly recognized as viable alternative biomarkers for direct diagnosis and prognosis of disease conditions, including various cancers. In this work, we addressed the problem of systematically developing an miRNA-based nomogram for the reliable prognosis of cervical cancer. Towards this, we preprocessed public-domain miRNA -omics data from cervical cancer patients, and applied a cascade of filters in the following sequence: (i) differential expression criteria with respect to controls; (ii) significance with univariate survival analysis; (iii) passage through dimensionality reduction algorithms; and (iv) stepwise backward selection with multivariate Cox modeling. This workflow yielded a compact prognostic DEmiR signature of three miRNAs, namely hsa-miR-625-5p, hs-miR-95-3p, and hsa-miR-330-3p, which were used to construct a risk-score model for the classification of cervical cancer patients into high-risk and low-risk groups. The risk-score model was subjected to evaluation on an unseen test dataset, yielding a one-year AUROC of 0.84 and five-year AUROC of 0.71. The model was validated on an out-of-domain, external dataset yielding significantly worse prognosis for high-risk patients. The risk-score was combined with significant features of the clinical profile to establish a predictive prognostic nomogram. Both the miRNA-based risk score model and the integrated nomogram are freely available for academic and not-for-profit use at CESCProg, a web-app (<https://apalania.shinyapps.io/cescprog>).

14 ABSTRACT

15 Cervical squamous cell carcinoma, more commonly cervical cancer, is the fourth common
16 cancer among women worldwide with substantial burden of disease, and less-invasive, reliable
17 and effective methods for its prognosis are necessary today. Micro-RNAs are increasingly
18 recognized as viable alternative biomarkers for direct diagnosis and prognosis of disease
19 conditions, including various cancers. In this work, we addressed the problem of systematically
20 developing an miRNA-based nomogram for the reliable prognosis of cervical cancer. Towards
21 this, we preprocessed public-domain miRNA -omics data from cervical cancer patients, and
22 applied a cascade of filters in the following sequence: (i) differential expression criteria with
23 respect to controls; (ii) significance with univariate survival analysis; (iii) passage through
24 dimensionality reduction algorithms; and (iv) stepwise backward selection with multivariate Cox
25 modeling. This workflow yielded a compact prognostic DEmiR signature of three miRNAs,
26 namely hsa-miR-625-5p, hs-miR-95-3p, and hsa-miR-330-3p, which were used to construct a
27 risk-score model for the classification of cervical cancer patients into high-risk and low-risk
28 groups. The risk-score model was subjected to evaluation on an unseen test dataset, yielding a
29 one-year AUROC of 0.84 and five-year AUROC of 0.71. The model was validated on an out-of-
30 domain, external dataset yielding significantly worse prognosis for high-risk patients. The risk-
31 score was combined with significant features of the clinical profile to establish a predictive
32 prognostic nomogram. Both the miRNA-based risk score model and the integrated nomogram
33 are freely available for academic and not-for-profit use at CESCProg, a web-app
34 (<https://apalania.shinyapps.io/cescprog>).

35

36 INTRODUCTION

37 Cervical cancer (cervical squamous cell carcinoma; CESC) ranks fourth globally among cancers
38 in women, and second among women of reproductive age. Due to unequal implementation of
39 invasive screening techniques, the morbidity and mortality rate of cervical cancer continues to
40 rise in countries like India, where it accounted for 9.4% of all cancers and 18.3% of new cases in
41 2020¹. Multiple etiological factors contribute to its incidence, including persistent infection of
42 human papilloma virus (HPV)², and known lifestyle factors such as excessive smoking and use

43 of contraceptive pills. Cervical cancer tends to be refractory to treatment unless detected early,
44 and its prognosis is vital to quality-of-life expectations. Late diagnoses in the advanced stages of
45 cervical cancer require expensive and complex treatment, with concomitant poor prognoses³.
46 Many gaps remain with respect to cervical cancer screening, diagnosis and prognosis⁴, and
47 biomarkers with high specificity and sensitivity are necessary.

48 MiRNAs exert key control over regulation of gene expression⁵, by inducing specific translational
49 repression via target mRNA 3' UTR deadenylation and decapping. MiRNAs are known to target
50 ~60% of the transcriptome, thus modulating biological processes⁶. Their aberrant, differential
51 expression is implicated in various cancers, where they act as either oncogenes (oncomirs) or
52 tumor suppressor genes (mirsupps), regulating tumorigenic process like cell maturation, cell
53 proliferation, migration, invasion, apoptosis, and metastasis⁷. MiRNA biomarkers from the
54 serum or cervical mucus could potentially augment systems for early diagnosis, prediction of
55 disease progression, and outcome improvement, in addition to facilitating prognostic
56 information, with respect to cervical cancer. The US National Cancer Institute launched the
57 Cancer Genome Atlas (TCGA) to characterize different tumor types using -omics platforms, and
58 make raw and processed data available to all researchers⁸. In this study, we used the TCGA
59 CESC miRNA -omics dataset to build a validated prognostic risk model and predictive
60 nomogram based on a minimal miRNA signature and the clinical profile. The developed models
61 have been deployed as a freely-available web-app service for non-commercial use at CESCProg
62 (<https://apalania.shinyapps.io/cescprog>).

63 MATERIALS AND METHODS

64 The workflow is summarised in Fig. 1, and discussed in detail below.

65 Data preprocessing

66 Normalized and log₂-transformed Illumina HiSeq miRSeq data preprocessed with the TCGA
67 miRNA analysis pipeline were obtained from firebrowse.org portal⁹. The patient barcode of each
68 sample was parsed to annotate the samples as 'normal' and 'cancer'. The corresponding clinical
69 metadata was also retrieved from firebrowse.org
70 (CESC.Merge_Clinical.Level_1.2016012800.0.0.tar) and used to annotate the stage information
71 (encoded in 'patient.stage_event.clinical_stage' variable) of the tumor samples, and then merged

72 with the expression data. The clinical stage is essentially the surgical stage prior to any treatment
73 received, from the biopsy obtained at the time of surgery. Collapsing possible substages (A, B,
74 C) in each stage yielded the four-class macro-progression of stages (I, II, III, IV). Certain
75 demographic and clinical factors in the metadata including age, HPV status, smoking history,
76 pregnancies, histologic grade, vital status and were retained. Based on the merged dataset,
77 miRNAs with negligible change in expression across samples (expression $\sigma < 1$) were removed,
78 as were samples with absent stage information. R (www.r-project.org) was used for dataset
79 preprocessing.

80 **Linear modelling**

81 The miRNA expression analyses of cancer stages relative to the normal tissue (controls) were
82 performed using the limma package in R¹⁰. The workflow was essentially adapted from earlier
83 protocols developed in our lab¹¹. To recapitulate, a linear model was fit using controls as
84 intercept and sample stages as indicator variables. The fit model was adjusted with empirical
85 Bayes to obtain moderated t-statistics¹². Multiple hypothesis testing and the false discovery rate
86 were applied using the method of Hochberg and Benjamini to yield adjusted p-values of the F-
87 statistic of the linear fit¹³. Based on the fold change (FC) in the expression of individual miRNAs
88 across conditions, miRNAs with $|\log_2(\text{FC})| > 2.0$ and adj. p-value < 0.05 were considered
89 significantly differentially expressed miRNAs (DEmiRs). The preprocessed dataset was then
90 split into train and test datasets in the ratio 0.8:0.2. The test dataset was used for the performance
91 evaluation of the final model, but kept invisible to the model development process.

92 **Development of compact miRNA signature**

93 Univariate Cox models¹⁴ were used to screen the DEmiRs by significance, and only DEmiRs
94 with p-value < 0.05 were filtered for further analysis. Two robust feature selection methods,
95 namely Least absolute shrinkage and selector operation (LASSO) Cox regression¹⁵ and Support
96 vector machine - recursive feature elimination (SVM-RFE)¹⁶, were used in combination to
97 reduce the dimensionality of the prognostic DEmiRs. LASSO, a form of ‘penalized’ regression
98 with L1 penalty, was implemented using R-glmnet¹⁷, whereas SVM-RFE, which computes
99 ranking weights for all features and then iteratively performs backward selection, was
100 implemented using R-e1071¹⁸. A union of the features selected from these two implementations

101 was taken forward and used in a stepwise multivariate Cox logistic regression¹⁹ for establishing
102 the prognostic DEmiR signature of cervical cancer.

103 **Prognostic risk model**

104 A risk model was formulated based on the identified prognostic DEmiR signature and used to
105 evaluate the survival risk of each patient. It is given by the exponent in the multivariate Cox
106 model:

$$107 \text{ miRNA_Risk_score} = \beta_1 \times \text{miRNA}_1 + \beta_2 \times \text{miRNA}_2 + \dots + \beta_n \times \text{miRNA}_n \quad \text{--- (1)}$$

108 where n is the size of the prognostic DEmiR signature, miRNA_i denotes the expression level of
109 the i^{th} miRNA, and β_i denotes the effect-size (or weight) of the i^{th} miRNA. Applying the optimal
110 cut-point (i.e, median) given by `maxstat` (maximally selected rank) statistic from the R-
111 `survminer`²⁰ to the risk score distribution, we categorized (binarized) patients with CESC into
112 high-risk and low-risk groups. Kaplan-Meier curves and AUROC were used to analyze the
113 overall survival (OS) probabilities between high-risk and low-risk groups using R `Survival`²¹ and
114 R `survivalROC`²², respectively. The test dataset and an additional external dataset for blind
115 validation were used to evaluate the prognostic value of the developed model.

116 **Nomogram construction**

117 Since miRNA-based risk score was unlikely to be the only prognostic predictor for overall
118 survival, the clinical profile was also considered. Both univariate and multivariate Cox
119 regression analyses were performed with some clinical features, namely age, pregnancies,
120 `smoking_history`, grade, stage, and `HPV_status`. Only those clinical variables that survived both
121 the analyses were used with the miRNA-based risk score to build an integrated nomogram map
122 that tabulates the probability of one-year and five-year OS of CESC. The discrimination was
123 quantified using Harrell's concordance index (C-index), and calibration performed using
124 bootstrap with 1000 resamples.

125 **RESULTS**

126 The TCGA expression data consisted of expression values of 2589 miRNA in 312 samples
127 enrolled in this study, including 309 cervical cancer tissues and 3 matched normal tissues. Post

128 data preprocessing, we obtained an expression dataset consisting of 467 miRNAs across 303
129 samples with stage annotation. Table 1 shows the distribution of samples according to the AJCC
130 staging system²³. The demographic features and clinical characteristics considered, namely age,
131 smoking history, vital status, pregnancies, HPV status, and histologic grade are summarized in
132 Table 2. Fitting the linear model and applying the filter criteria yielded a total of 101
133 differentially expressed miRNAs between cervical cancer tissues and matched normal tissues,
134 provided in Supplementary File S1. Most of the top-ranked miRNAs are overexpressed (for e.g,
135 hsa-miR-200c-3p, hsa-miR-141, hsa-miR-200a, hsa-miR-21-5p), suggesting oncomir function
136 with increased epigenetic suppression of target tumor-suppressor gene expression. Table 3 shows
137 the top ten miRNAs with their stage-wise log₂FC and linear model significance.

138 Each DEmiR was subjected to univariate Cox modeling to evaluate its prognostic significance.
139 This process identified only 52 miRNAs as significantly associated with overall survival, based
140 on p-value < 0.05 (data presented in Supplementary File S2). To optimize the dimensions of the
141 prognostic miRNA biomarker panel, we applied Lasso-penalized Cox regression on the 52
142 miRNAs to obtain five miRNAs, hsa-miR-625-5p, hsa-miR-3934-5p, hsa-miR-330-3p, hsa-miR-
143 642a-5p, has-miR-95-3p, Only one miRNA, hsa-miR-616-5p, survived the SVM-RFE feature
144 selection process. Figure 2 shows the union of these results (i.e, the six miRNAs).

145 The six miRNAs were taken forward for multivariate survival analysis, and subjected to a
146 stepwise backward-selection process, to further compact the miRNA signature. This process
147 yielded an optimal signature of three miRNAs namely hsa-miR-625-5p, hsa-miR-330-3p, and
148 hsa-miR-95-3p, with model p-value < 0.002 (Table 4), for construction of the CESC prognostic
149 risk model.

150 The CESC prognostic risk model, given by eqn. (1), was then parameterized using the expression
151 of these three miRNAs:

$$152 \text{ miRNA_Risk_score} = 0.30*\text{hsa-miR-95-3p} + 0.35*\text{hsa-miR-330-3p} - 0.52*\text{hsa-miR-625-5p}$$

153 — (2)

154 It is seen that hsa-miR-625-5p has a significant protective effect on CESC OS, whereas the
155 expression of hsa-miR-95-3p and hsa-miR-330-3p elevate the risk. Based on this model, we
156 computed the risk score for each patient in the train dataset, and used the maxstat of the resulting

157 risk-score distribution to separate patients into high- and low-risk groups (Figure 3A). The
158 Kaplan–Meier survival curve of this distribution revealed significantly worse prognosis in the
159 high-risk group (p -value $< 1E-4$) (Figure 3B). Time-dependent ROC analysis of the risk-score
160 model on the train dataset for 1-, 2-, 3-, and 5-year overall survival yielded prognostic AUC
161 values of 0.71, 0.72, 0.74 and 0.73, respectively (Figure 3C). These results encouraged validation
162 of the CESC-related prognostic signature on the test dataset, whose risk-score distribution is
163 shown in Figure 4A. The following outcomes validated the results: (i) Kaplan-Meier survival
164 curve showed significantly worse prognosis in the high-risk group (p -value $< 1E-4$) (Figure 4B) ;
165 and (ii) time-dependent AUROC values 0.84, 0.79, 0.71 and 0.71 were obtained for 1-, 2-, 3-,
166 and 5-year overall survival, respectively (Figure 4C).

167 To validate the prognostic value of the model on an external, out-of-domain dataset, we used the
168 study results of How et al²⁴. This study used a TaqMan Low Density Array (TLDA) to measure
169 expression in formalin-fixed paraffin-embedded (FFPE) cervix samples. Two datasets from the
170 study were used:

171 (i) Normalized and \log_2 -transformed miRNA expression data of 87 FFPE cervix samples used
172 for validation, available at:
173 <https://www.ncbi.nlm.nih.gov/pmc/articles/PMC4399941/bin/pone.0123946.s005.txt> ; and

174 (ii) corresponding clinical information, available at:
175 <https://www.ncbi.nlm.nih.gov/pmc/articles/PMC4399941/bin/pone.0123946.s002.xlsx>. The

176 clinical information was used to annotate the samples, and the expression subset corresponding
177 to the three miRNAs in the optimal risk model (i.e. eqn. 2) was extracted. Since the miRNA arm
178 information (-3p or -5p) was missing for hsa-miR-625 and hsa-miR-95, the arm-neutral
179 expression values for both these miRNAs were used. The risk score for each sample was
180 calculated based on eqn. 2, and the resulting risk score distribution was stratified into high-risk
181 and low-risk patient groups based on the maxstat statistic computed by R survminer. The curves
182 were visualized using Kaplan-Meier analysis, yielding significantly worse prognosis ($P < 0.032$)
183 in the high-risk patient group relative to the low-risk group (Figure 5).

184 Certain clinical features namely age, HPV_status, pregnancies, smoking_history,
185 histologic_grade, and stage could boost the prognostic predictive value, and hence were
186 examined for candidate inclusion in the risk model. Each clinical feature was subjected to the

187 univariate Cox survival analysis, and only one clinical feature turned out significant, namely the
188 stage. This was used with the miRNA-based risk-score to model an integrated multivariate Cox
189 logistic regression. Both the factor levels of both the variables were significant, and the overall
190 multivariate model was extremely significant (p-value $\sim 4E-05$) (Figure 6). The integrated CESC
191 prognostic risk model was then parameterized as:

$$192 \text{ Integrated_risk_score} = 0.64 * \text{miRNA_Risk_score} + 0.74 * \text{Stage} \quad \text{--- (3)}$$

193 Based on the risk models developed, a nomogram was built to predict one-year and five-year
194 survival probabilities (Figure 7). The nomogram C-index was estimated as 0.7136 ± 0.047 ,
195 indicating good discrimination. Further, the nomogram calibration plots for one-year and five-
196 year OS probabilities based on bootstrap resampling showed consistency between the predicted
197 and actual survival probabilities (Figure 8).

198 **DISCUSSION**

199 MiRNAs add a layer of critical regulatory control over genomic expression, and aberrations in
200 their expression could lead to the development of cancer hallmarks²⁵. MiRNAs could be detected
201 in the serum, and lend valuable potential as diagnostic and prognostic biomarkers of various
202 cancers, including cervical cancer²⁶. Several prognostic miRNAs for CESC have been reported,
203 including miR-31²⁷, miR-155²⁸, and miR425-5p²⁹. However a systematic hypothesis-free scan
204 for comprehensive miRNA signatures remains missing in the literature. In this study, we have
205 attempted to fill this void with an integrated multi-layered bioinformatics approach to the
206 detection of a reliable prognostic DEmiR biomarker signature. The study has yielded three
207 prognostic miRNAs, namely hsa-miR-625-5p, hsa-miR-95-3p, and hsa-miR-330-3p.
208 Downregulation of hsa-miR-625-5p has been documented in many cancers including bladder
209 cancer³⁰, non-small cell lung cancer³¹, hepatocellular carcinoma³², melanoma³³ and cervical
210 cancer³⁴. A causal mechanism relating miR-625-5p expression to inhibition of cervical cancer
211 cell growth via suppression of NF- κ B signaling has been reported³⁵, consistent with its mirsupp
212 identity disclosed here. Sponging miR-625-5p in turn is likely to drive cervical cancer
213 progression, and this has been demonstrated recently³⁶. Jafarzadeh et al. suggested that miR-330-
214 3p promoted pro-tumorigenic events in various cancers like lung cancer, pancreatic cancer,
215 bladder cancer and cervical cancer, and that its downregulation could stall tumor development³⁷,

216 both observations consistent with its oncomir identity disclosed here. Further, miR-95-3p has
217 been implicated in activating the wnt/ β catenin pathway in prostate cancer tissues³⁸, thereby
218 promoting cell proliferation, migration and invasion, consistent with its oncomir identity
219 disclosed here.

220 To examine the network-level effects of these miRNAs, we retrieved the RNA-Seq
221 transcriptome for each patient in our dataset from firebrowse.org, and correlated this data with
222 the expression of the three miRNAs of interest to infer potential target genes. Target genes with
223 substantial inverse correlation in expression (defined as Pearson ρ or Spearman ρ or Kendall $\tau <$
224 -0.3) were identified, and the consensus with multiMiR³⁹ predictions for each of the three
225 miRNAs was investigated. This yielded three consensus target genes with respect to hsa-miR-95-
226 3p, namely NXPH3, BOC, EID1; two consensus target genes with respect to hsa-miR-625-5p,
227 namely SIN3B and TPRG1L; and two consensus target genes with respect to hsa-miR-330-3p,
228 namely THRA and DYRK2. Functional enrichment analysis of the consensus genes conducted
229 with miRNet⁴⁰ on GO and KEGG databases yielded significance for cancer pathways and cell
230 cycle regulation. We also used the miR2Trait server⁴¹ to investigate the diseasome of this three-
231 miRNA signature, and found significance for ‘uterine cervical neoplasm’ (p-value $\sim 1.5E-3$),
232 ‘squamous cell carcinoma’ (p-value $\sim 7.7E-3$), and ‘cervical intraepithelial neoplasia’ (p-value
233 $\sim 2.2E-2$). Detailed results of the above investigations are presented in Supplementary File S3.

234 Nomograms are widely used for simplifying the task of interpretation from models, and have
235 been constructed with miRNAs for cervical cancer screening⁴², prognosis⁴³, and recurrence
236 risk⁴⁴. To facilitate the ready prognosis of cervical cancer patients, the models developed in this
237 work were re-built with the full (train + test) dataset, and served as a web-app named CESCProg,
238 deployed at: <https://apalania.shinyapps.io/cescprog/> for non-commercial uses. The concerned
239 user may provide the form inputs, namely the expression values of the three prognostic DE miRs
240 and an optional sample staging information. Based on the user request, the app proceeds to
241 classify the risk of the sample, and compute a risk-score based on eqn. 2 or eqn. 3. The
242 calculated risk-score is then consulted with the back-end nomogram to estimate the one-year and
243 five-year survival probabilities. Serum-based or cervical mucus-based miRNAs are minimally
244 invasive, and could be detected and quantified using a range of techniques (for e.g, see ref. 45).

245 CONCLUSIONS

246 MiRNA biomarkers are an emerging diagnostic and prognostic aid to the management of
247 disease, especially cancers. Here we present CESCProg, an miRNA-based prognostic model for
248 cervical cancer developed by applying a sequence of purifying filters to the TCGA CESC
249 dataset. All the three miRNAs in the panel, namely hsa-miR-95-3p, hsa-miR-330-3p and hsa-
250 miR-625-5p, show upregulation in cervical cancer relative to controls, suggesting feasibility for
251 detection as biomarkers. In the miRNA risk model, hsa-miR-625-5p exhibits a protective effect
252 on OS, while the other two miRNAs elevate the risk. The miRNA risk model was effective and
253 extremely significant in stratifying CESC OS on the test dataset. A second risk model was
254 developed with the inclusion of clinical features to maximize nomogram discrimination. This
255 yielded a C-index of 0.7136 ± 0.047 . The models have been deployed as a web-service as a
256 possible aid to medical decision-making. They are available for non-profit use at:
257 <https://apalania.shinyapps.io/cescprog> .

258 **ACKNOWLEDGMENTS**

259 We would like to thank the School of Chemical and Biotechnology & CeNTAB, SASTRA
260 Deemed University, for computing and infrastructure support.

261 **REFERENCES**

- 262 1. Sung, H. *et al.* Global Cancer Statistics 2020: GLOBOCAN Estimates of Incidence and
263 Mortality Worldwide for 36 Cancers in 185 Countries. **71**, 209-249,
264 doi:<https://doi.org/10.3322/caac.21660> (2021).
- 265 2. Bruni *et al.* ICO/IARC Information Centre on HPV and Cancer (HPV Information
266 Centre). Human Papillomavirus and Related Diseases in India. Summary Report 22 October
267 2021.
- 268 3. Mehrotra, R. & Yadav, K. Cervical Cancer: Formulation and Implementation of Govt of
269 India Guidelines for Screening and Management. *Indian Journal of Gynecologic Oncology* **20**, 4,
270 doi:[10.1007/s40944-021-00602-z](https://doi.org/10.1007/s40944-021-00602-z) (2021).
- 271 4. Jiang, Y. *et al.* Identification of Circulating MicroRNAs as a Promising Diagnostic
272 Biomarker for Cervical Intraepithelial Neoplasia and Early Cancer: A Meta-Analysis. *BioMed*
273 *research international* **2020**, 4947381, doi:[10.1155/2020/4947381](https://doi.org/10.1155/2020/4947381) (2020).

- 274 5. Li, Z. & Rana, T. Therapeutic targeting of microRNAs: current status and future
275 challenges. *Nature reviews drug discovery* **13**, 622-638 (2014).
- 276 6. Pedroza-Torres, A. *et al.* A microRNA expression signature for clinical response in
277 locally advanced cervical cancer. *Gynecologic oncology* **142**, 557-565,
278 doi:10.1016/j.ygyno.2016.07.093 (2016).
- 279 7. Reddy, K. B. MicroRNA (miRNA) in cancer. *Cancer Cell International* **15**, 38,
280 doi:10.1186/s12935-015-0185-1 (2015).
- 281 8. Chandran, U. R. *et al.* TCGA Expedition: A Data Acquisition and Management System
282 for TCGA Data. *PloS one* **11**, e0165395, doi:10.1371/journal.pone.0165395 (2016).
- 283 9. Deng M, Brägelmann J, Kryukov I, Saraiva-Agostinho N, Perner S. FirebrowseR: an R
284 client to the Broad Institute's Firehose Pipeline. Database (Oxford). doi:
285 10.1093/database/baw160 (2017).
- 286 10. Ritchie, M. E. *et al.* limma powers differential expression analyses for RNA-sequencing
287 and microarray studies. *Nucleic Acids Research* **43**, e47-e47, doi:10.1093/nar/gkv007 %J
288 Nucleic Acids Research (2015).
- 289 11. Sarathi, A. & Palaniappan, A. Novel significant stage-specific differentially expressed
290 genes in hepatocellular carcinoma. *BMC cancer* **19**, 663, doi:10.1186/s12885-019-5838-3
291 (2019).
- 292 12. McCarthy, D. J. & Smyth, G. K. Testing significance relative to a fold-change threshold
293 is a TREAT. *Bioinformatics (Oxford, England)* **25**, 765-771, doi:10.1093/bioinformatics/btp053
294 (2009).
- 295 13. Hochberg, Y. & Benjamini, Y. More powerful procedures for multiple significance
296 testing. *Statistics in medicine* **9**, 811-818, doi:10.1002/sim.4780090710 (1990).
- 297 14. Clark, T. G., Bradburn, M. J., Love, S. B. & Altman, D. G. Survival analysis part I: basic
298 concepts and first analyses. *British journal of cancer* **89**, 232-238, doi:10.1038/sj.bjc.6601118
299 (2003).
- 300 15. Tibshirani, R. J. The lasso method for variable selection in the Cox model. *Statistics in*
301 *medicine* **16**, 385-395 (1997).
- 302 16. Adorada, A., Permatasari, R., Wirawan, P. W., Wibowo, A. & Sujiwo, A. in *2018 2nd*
303 *International Conference on Informatics and Computational Sciences (ICICoS)*. 1-4.

- 304 17. Friedman, J., Hastie, T. & Tibshirani, R. Regularization Paths for Generalized Linear
305 Models via Coordinate Descent. *Journal of statistical software* **33**, 1-22 (2010).
- 306 18. Dimitriadou, E., Hornik, K., Leisch, F., Meyer, D. & Weingessel, A. Vol. 1 (2009).
- 307 19. Bradburn, M. J., Clark, T. G., Love, S. B. & Altman, D. G. Survival analysis part II:
308 multivariate data analysis--an introduction to concepts and methods. *British journal of cancer* **89**,
309 431-436, doi:10.1038/sj.bjc.6601119 (2003).
- 310 20. Kassambara, A., Kosinski, M. & Biecek, P. JRpv: survminer: Drawing Survival Curves
311 using 'ggplot2'. 2017, 1.
- 312 21. Therneau, T. J. R. p. v. A package for survival analysis in S. **2** (2015).
- 313 22. Heagerty, Patrick J., Paramita Saha-Chaudhuri, and Maintainer Paramita Saha-
314 Chaudhuri. "Package 'survivalROC'." *San Francisco: GitHub* (2013).
- 315 23. Amin, M. B. *et al.* The Eighth Edition AJCC Cancer Staging Manual: Continuing to build
316 a bridge from a population-based to a more "personalized" approach to cancer staging. *CA: a*
317 *cancer journal for clinicians* **67**, 93-99, doi:10.3322/caac.21388 (2017).
- 318 24. How C, Pintilie M, Bruce JP, Hui AB, Clarke BA, Wong P, Yin S, Yan R, Waggott D,
319 Boutros PC, Fyles A, Hedley DW, Hill RP, Milosevic M, Liu FF. Developing a prognostic
320 micro-RNA signature for human cervical carcinoma. *PLoS One*. 16;10(4):e0123946. doi:
321 10.1371/journal.pone.0123946 (2015).
- 322 25. Iorio, M. V. & Croce, C. M. MicroRNA dysregulation in cancer: diagnostics, monitoring
323 and therapeutics. A comprehensive review. *EMBO molecular medicine* **9**, 852,
324 doi:10.15252/emmm.201707779 (2017).
- 325 26. Pisarska, J. & Baldy-Chudzik, K. MicroRNA-based fingerprinting of cervical lesions and
326 cancer. *Journal of clinical medicine* **9**, 3668 (2020).
- 327 27. Wang, N., Zhou, Y., Zheng, L. & Li, H. MiR-31 is an independent prognostic factor and
328 functions as an oncomir in cervical cancer via targeting ARID1A. *Gynecologic oncology* **134**,
329 129-137, doi:https://doi.org/10.1016/j.ygyno.2014.04.047 (2014).
- 330 28. Fang, H., Shuang, D., Yi, Z., Sheng, H. & Liu, Y. Up-regulated microRNA-155
331 expression is associated with poor prognosis in cervical cancer patients. *Biomedicine &*
332 *Pharmacotherapy* **83**, 64-69, doi:https://doi.org/10.1016/j.biopha.2016.06.006 (2016).
- 333 29. Sun, L. *et al.* MicoRNA-425-5p is a potential prognostic biomarker for cervical cancer.
334 *Annals of clinical biochemistry* **54**, 127-133, doi:10.1177/0004563216649377 (2017).

- 335 30. Deng, H. *et al.* LINC00511 promotes the malignant phenotype of clear cell renal cell
336 carcinoma by sponging microRNA-625 and thereby increasing cyclin D1 expression. *Aging* **11**,
337 5975 (2019).
- 338 31. Dao, R. *et al.* Knockdown of lncRNA MIR503HG suppresses proliferation and promotes
339 apoptosis of non-small cell lung cancer cells by regulating miR-489-3p and miR-625-5p.
340 *Pathology, research and practise* **216**, 152823 (2020).
- 341 32. Zhou X, Zhang CZ, Lu SX, Chen GG, Li LZ, Liu LL, et al.. miR-625 suppresses tumour
342 migration and invasion by targeting IGF2BP1 in hepatocellular carcinoma. *Oncogene*. (2015)
343 34:965–77. 10.1038/onc.2014.35
- 344 33. Zou Y, Wang S-S, Wang J. CircRNA_0016418 expedites the progression of human skin
345 melanoma via miR-625/YY1 axis. *Eur Rev Med Pharmacol Sci*. (2019) 23:10918–30.
346 10.26355/eurrev_201912_19795
- 347 34. Wang, L. *et al.* LINC00958 facilitates cervical cancer cell proliferation and metastasis by
348 sponging miR-625-5p to upregulate LRRC8E expression. *Journal of cellular biochemistry* **121**,
349 2500-2509 (2020).
- 350 35. Li, Y. *et al.* MicroRNA-625-5p Sponges lncRNA MALAT1 to Inhibit Cervical
351 Carcinoma Cell Growth by Suppressing NF- κ B Signaling. *Cell Biochemistry and Biophysics* **78**,
352 217-225, doi:10.1007/s12013-020-00904-7 (2020).
- 353 36. Li H, Zheng S, Wan T, Yang X, Ouyang Y, Xia H, Wang X. Circular RNA circ_0000212
354 accelerates cervical cancer progression by acting as a miR-625-5p sponge to upregulate PTP4A1.
355 *Anticancer Drugs*. 19. doi: 10.1097/CAD.0000000000001435 (2022).
- 356 37. Jafarzadeh, A. *et al.* Dysregulated expression and functions of microRNA-330 in cancers:
357 A potential therapeutic target. *Biomedicine & Pharmacotherapy* **146**, 112600,
358 doi:10.1016/j.biopha.2021.112600 (2022).
- 359 38. Xi, M. *et al.* MicroRNA-95-3p promoted the development of prostatic cancer via
360 regulating DKK3 and activating Wnt/ β -catenin pathway. *Medical and Pharmacological Sciences*
361 **23**, 1002-1011 (2019).
- 362 39. Ru, Y. *et al.* The multiMiR R package and database: integration of microRNA-target
363 interactions along with their disease and drug associations. *Nucleic Acids Res* **42**, e133,
364 doi:10.1093/nar/gku631 (2014).

- 365 40. Chang, L., Zhou, G., Soufan, O. & Xia, J. miRNet 2.0: network-based visual analytics for
366 miRNA functional analysis and systems biology. *Nucleic Acids Research* **48**, W244-W251,
367 doi:10.1093/nar/gkaa467 (2020).
- 368 41. Babu P, Palaniappan A. miR2Trait: an integrated resource for investigating miRNA-
369 disease associations. PeerJ 10:e14146 <https://doi.org/10.7717/peerj.14146> (2022)
- 370 42. Kotani, K. *et al.* Nomogram for predicted probability of cervical cancer and its precursor
371 lesions using miRNA in cervical mucus, HPV genotype and age. *Scientific Reports* **12**, 16231,
372 doi:10.1038/s41598-022-19722-3 (2022).
- 373 43. Liu, J. *et al.* A microRNA–Messenger RNA Regulatory Network and Its Prognostic
374 Value in Cervical Cancer. *DNA and cell biology* **39**, 1328-1346, doi:10.1089/dna.2020.5590
375 (2020).
- 376 44. Bogani, G. *et al.* Nomogram-based prediction of cervical dysplasia
377 persistence/recurrence. *European journal of cancer prevention : the official journal of the*
378 *European Cancer Prevention Organisation (ECP)* **28**, 435-440,
379 doi:10.1097/cej.0000000000000475 (2019).
- 380 45. Baabu PRS, Srinivasan S, Nagarajan S, Muthamilselvan S, Selvi T, Suresh RR,
381 Palaniappan A. End-to-end computational approach to the design of RNA biosensors for
382 detecting miRNA biomarkers of cervical cancer. *Synth Syst Biotechnol.* **7(2)**, 802-814. doi:
383 10.1016/j.synbio.2022.03.008 (2022).

Figure 1

The workflow used in this study for the development of a compact validated risk model for cervical cancer prognosis.

The predictive prognostic nomogram was re-built with the full dataset prior to deployment at CESC-PROG (<https://apalania.shinyapps.io/cescprog>).

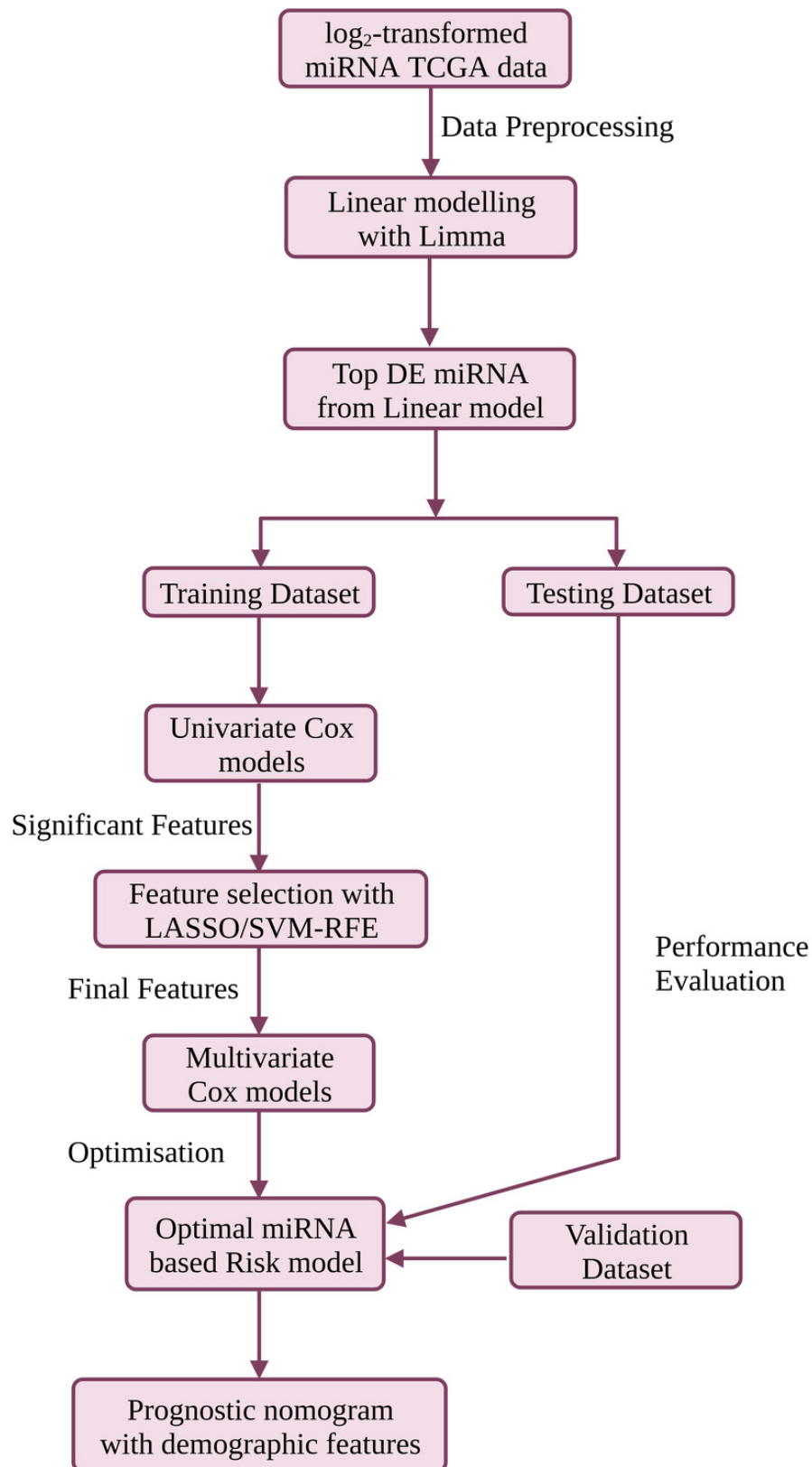


Figure 2

Volcano plot of the expression distribution of the miRNAs with non-trivial expression patterns in cancer samples relative to controls, highlighting the upregulated and downregulated DEmiRs, and the prognostic DEmiRs post the feature selection process.

All the prognostic DEmiRS were upregulated, but none were an outlier DEmiR (top right). X-axis denotes $\log_2(\text{FC})$ of expression with respect to control, and the Y-axis denotes the $-\log_{10}$ transformation of the p-value significance of the linear model for the respective miRNA.

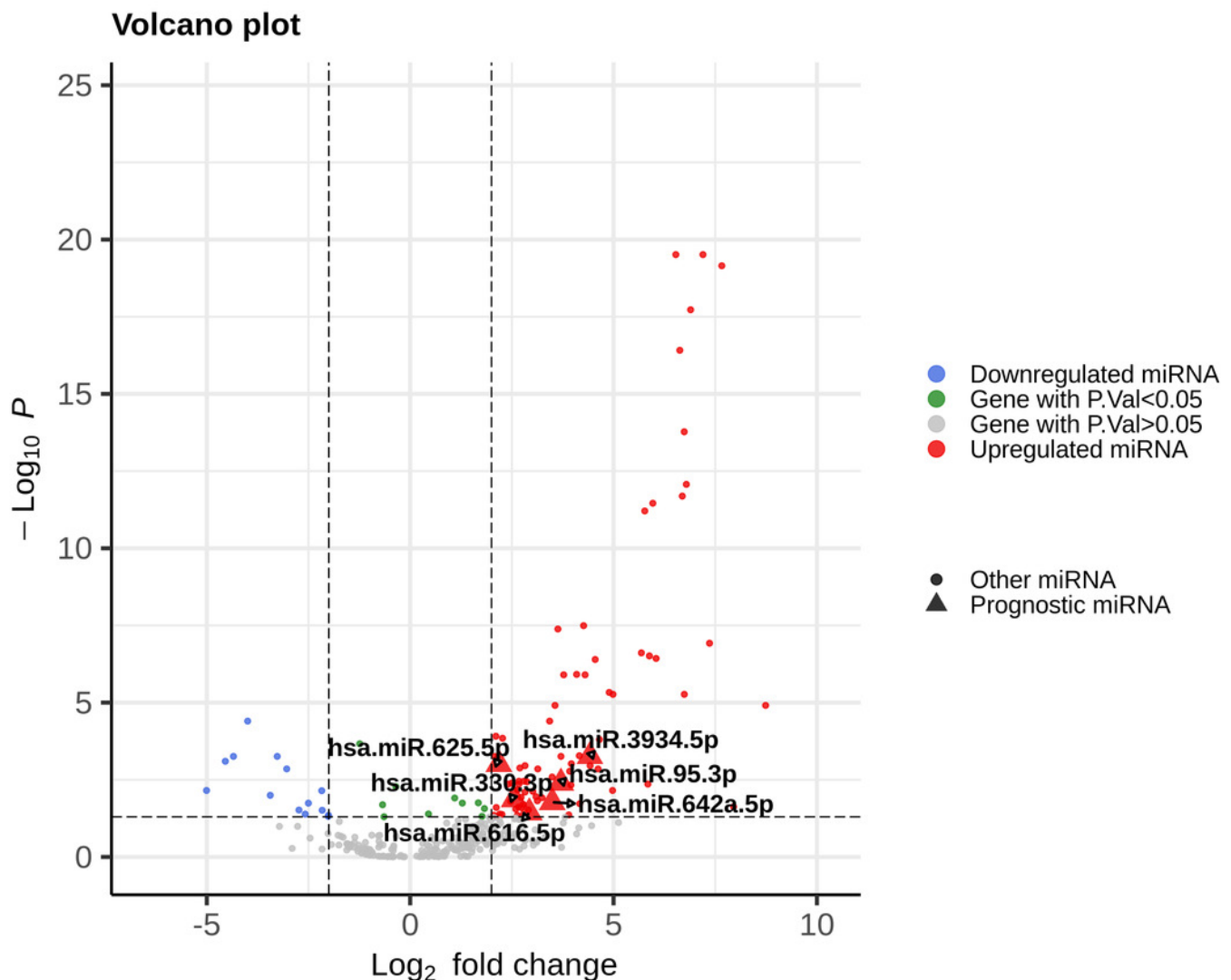


Figure 3

Performance of the constructed risk-score model on train dataset.

(A) This panel shows the risk-score value (top), survival status (middle), and expression of the three prognostic miRNAs (bottom) for each patient, sorted by the risk-score distribution. Patients were stratified into low-risk (blue) and high-risk (red) groups according to the risk-score value. The patterns in the expression profiles accord with the signed risk of the respective miRNAs. (B) Kaplan-Meier survival curves based on the three-miRNA prognostic signature showing significant difference between the two groups. (C) Time-dependent ROC curves for 1-, 2-, 3-, and 5-year overall survival predictions using the given model.

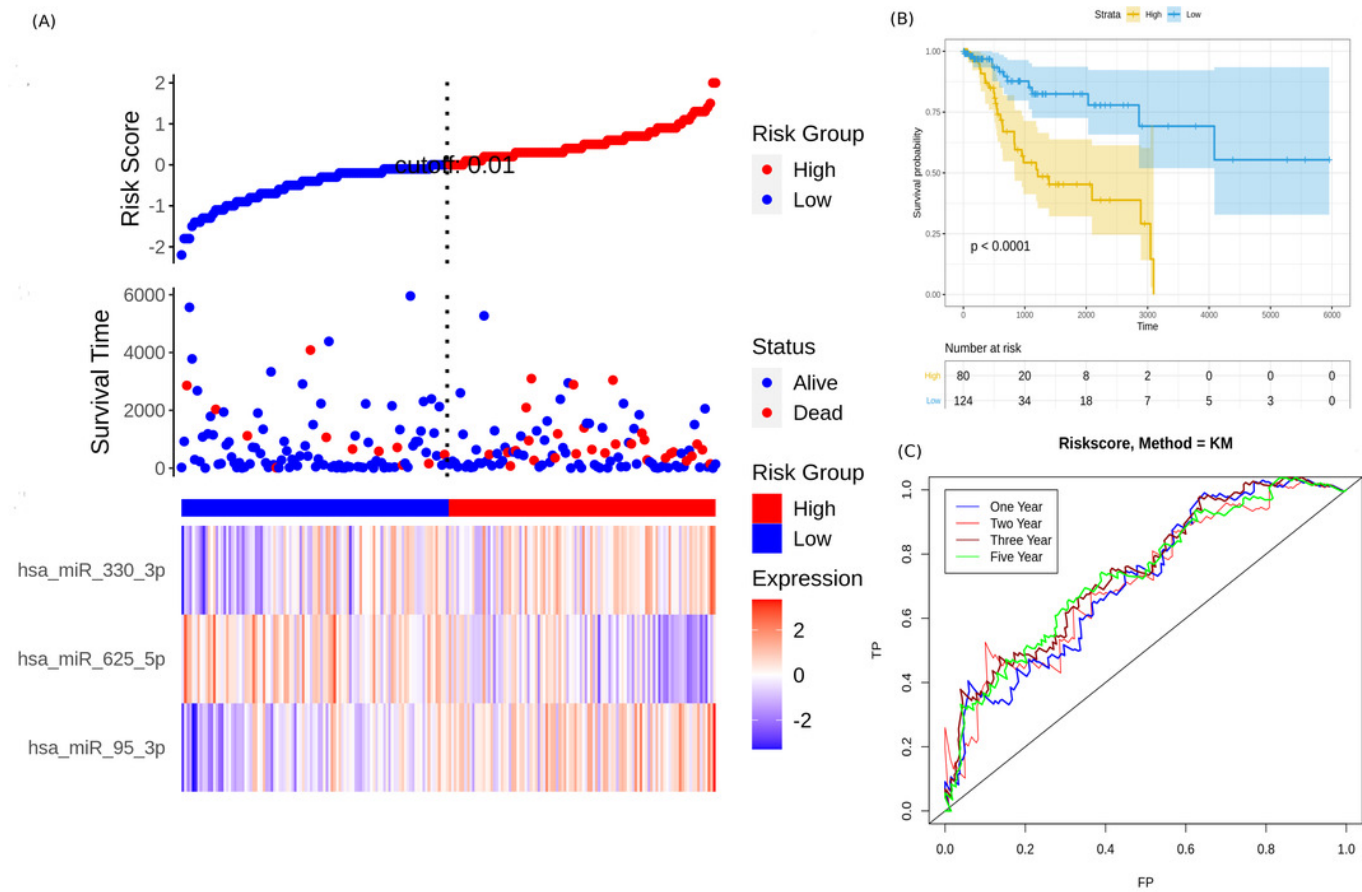


Figure 4

Performance evaluation of the constructed risk-score model on unseen test dataset.

(A) This panel shows the risk-score value (top), survival status (middle), and expression of the three prognostic miRNAs (bottom) for each patient, sorted by the risk-score distribution. Patients were stratified into low-risk (blue) and high-risk (red) groups according to the median risk-score value. (B) Kaplan-Meier survival curves based on the three-miRNA prognostic signature showing significant difference between the two groups. (C) Time-dependent ROC curves for 1-, 2-, 3-, and 5-year overall survival predictions using the given model.

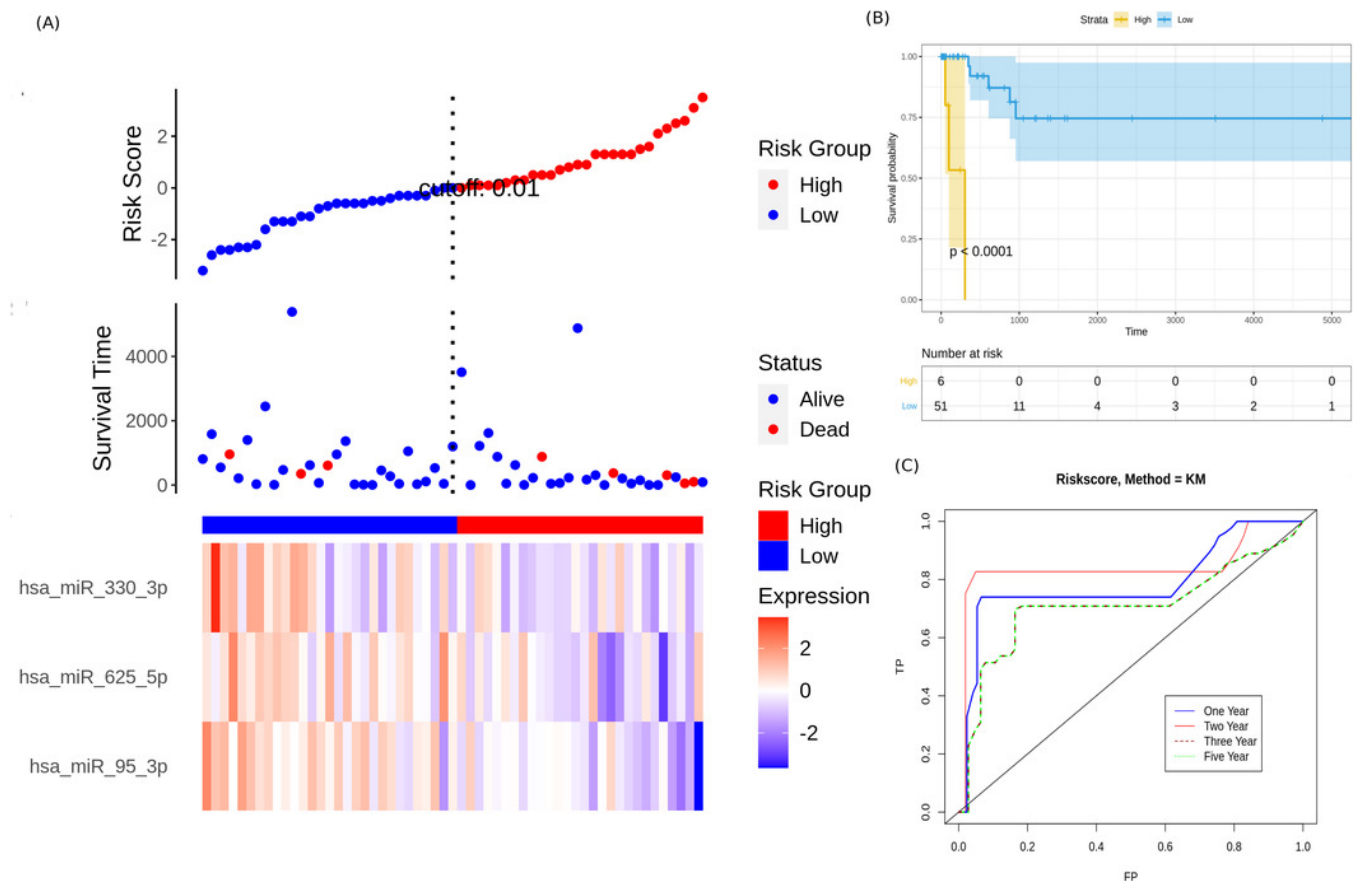


Figure 5

Kaplan-Meier survival curves for the validation dataset, showing significantly worse prognosis for the high-risk patient group relative to the low-risk group.

95% confidence bands for the risk groups are also shown.

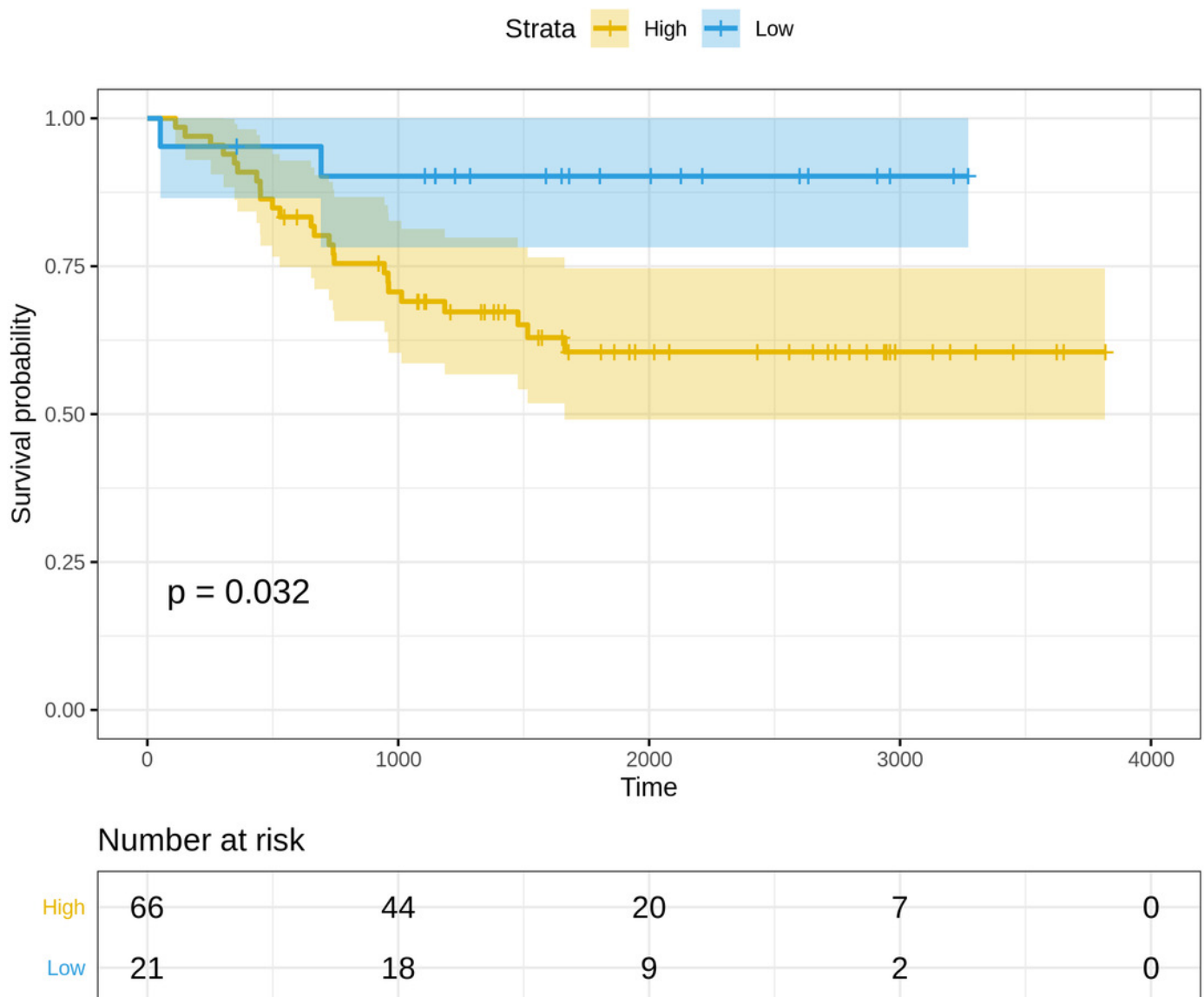
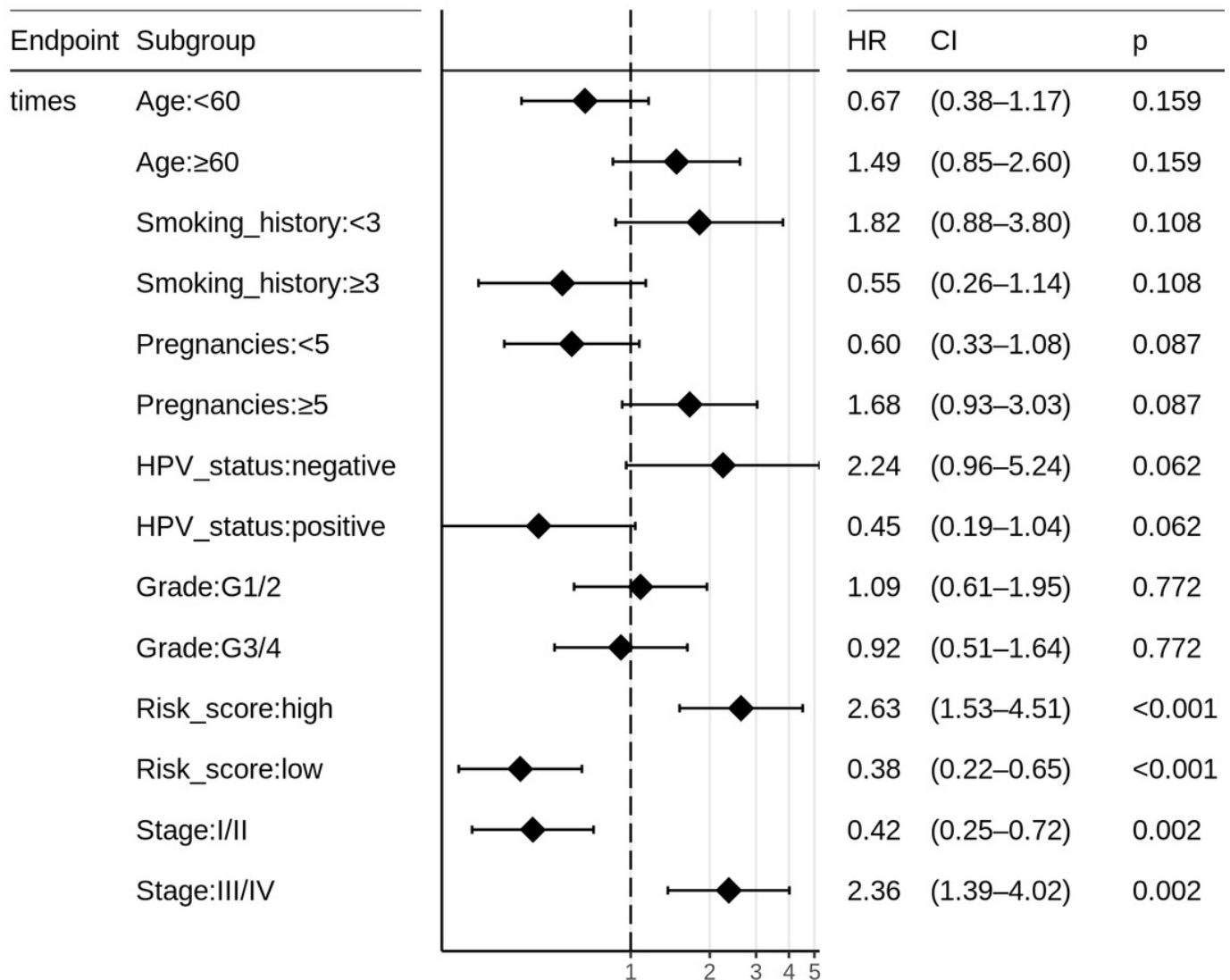


Figure 6

Univariate and multivariate Cox logistic regression analyses of patient clinical profile, with respect to CESC OS.

Surprisingly, neither the patient HPV-status nor tumor Grade is significant to CESC OS. However the distinction between early clinical stage (Stage:I/II) and late clinical stage (Stage:III/IV) cancers is significant, and constitutes an independent risk factor together with miRNA_risk_score.

Univariate Analysis



Multivariate Analysis

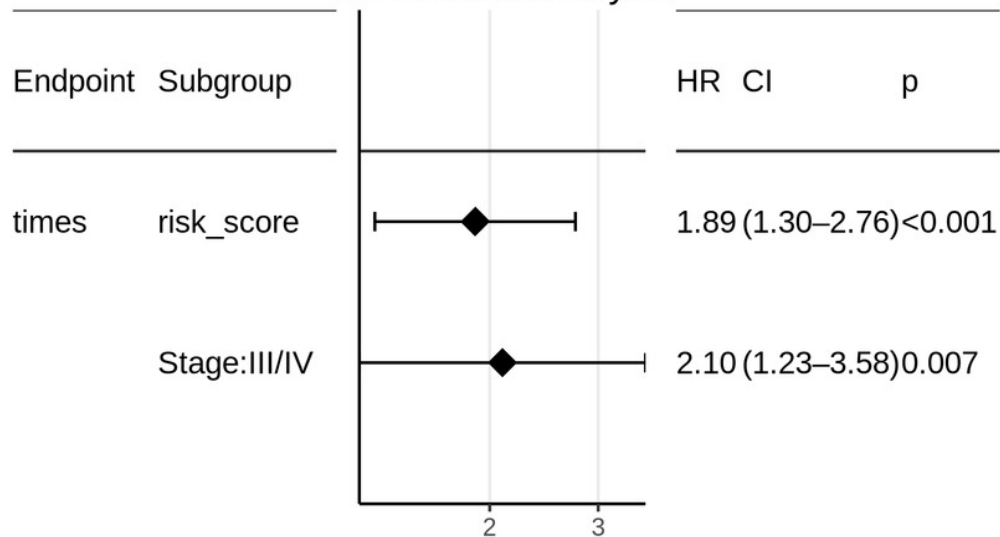


Figure 7

Nomogram for reading the overall survival in CESC sample, according to miRNA_risk_score (eqn. 2) and clinical stage.

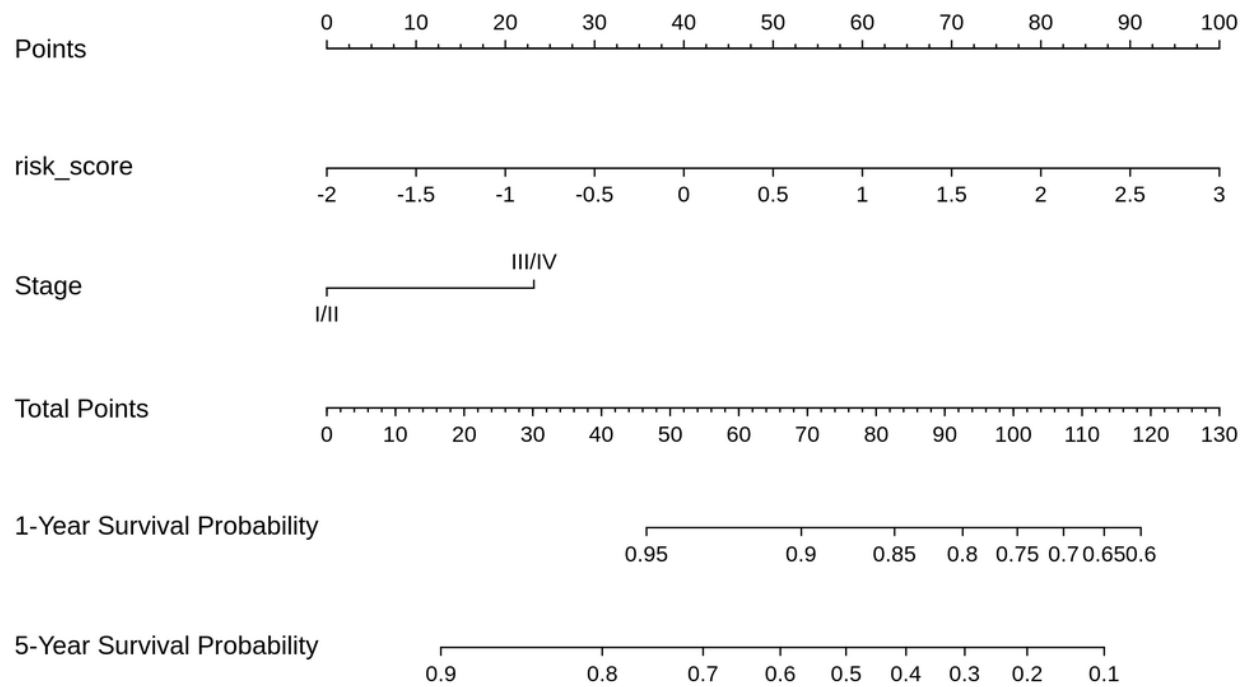


Figure 8

Nomogram calibration curves.

(A) 1-year OS probability; (B) 5-year OS probability. The four sub-cohorts of the dataset are visualized, and the corresponding x represents the bootstrap-corrected estimates of the nomogram performance along with the standard error. The solid line compares the nomogram performance with the reference truth.

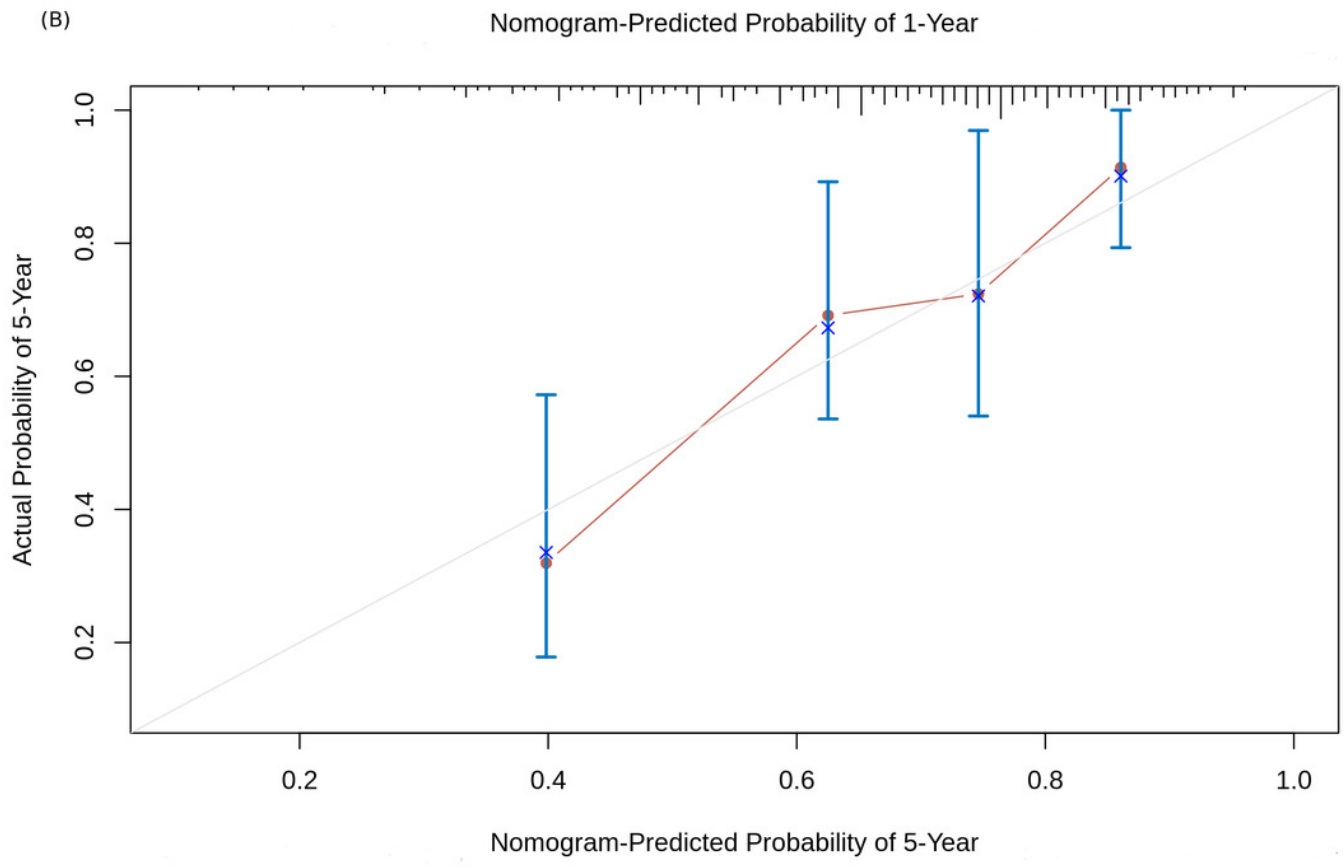
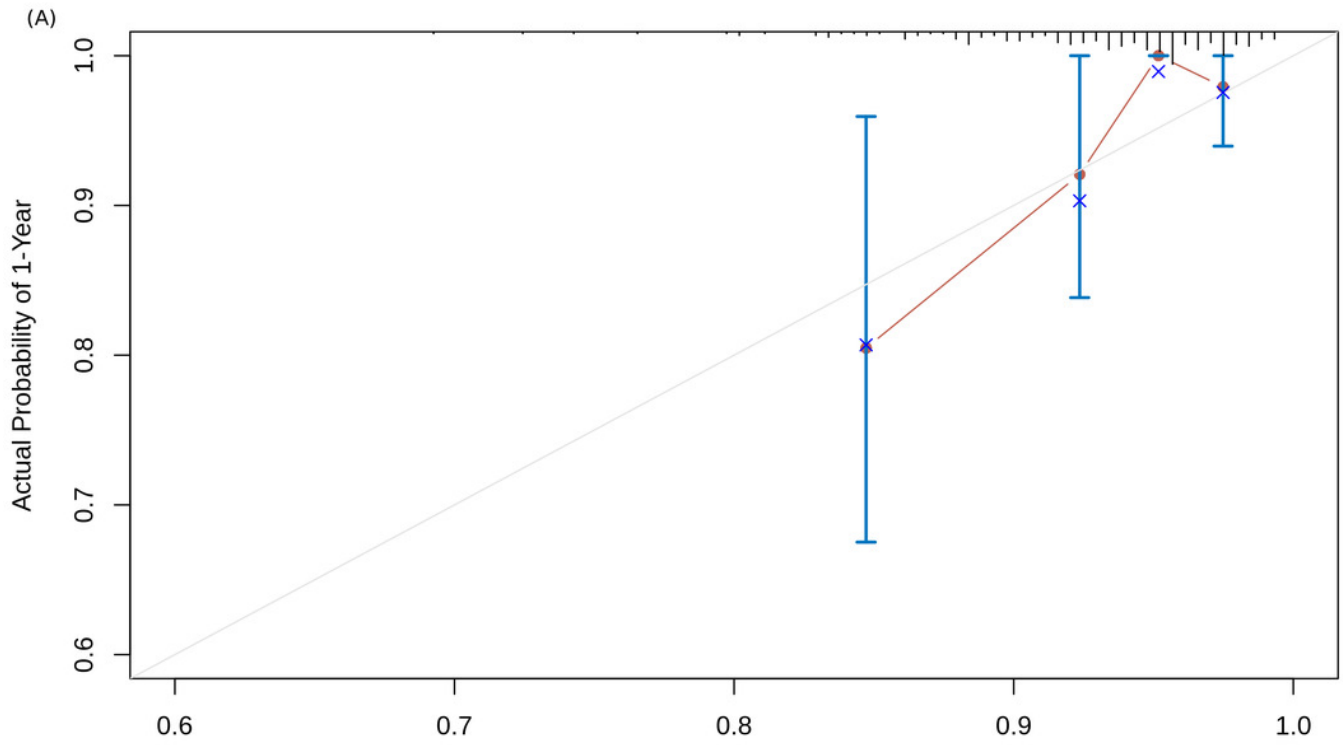


Table 1 (on next page)

Distribution of cases by stage.

AJCC staging is represented by the TNM (Tumor-Node-Metastasis) code. Control refers to matched normal samples, and 'NA' denotes cases with unavailable stage information.

TCGA stage	TNM classification	#Cases	
1	T1N0M0	5	163
1A	T1aN0M0	1	
1A1	T1a1N0M0	1	
1A2	T1a2N0M0	1	
1B	T1bN0M0	38	
1B1	T1b1N0M0	78	
1B2	T1b2N0M0	39	
2	T2N0M0	5	70
2A	T2aN0M0	9	
2A1	T2a1N0M0	5	
2A2	T2a2N0M0	7	
2B	T2bN0M0	44	
3	T3N0M0	1	46
3A	T3aN0M0	3	
3B	T3bN(any)M0	42	
4A	T4N(any)M0	9	21
4B	T(any)N(any)M1	12	
Control	-	3	
NA	-	7	

Table 2 (on next page)

Clinical profile of cervical cancer patients.

Summary of key clinical / demographic features of the dataset. For ordinal / continuous variables (age, smoking_history, and pregnancies), the mean \pm standard deviation is given. Histologic grade refers to the degree of differentiation in the cancer sample. It is seen that most cervical cancer patients present with HPV+ status.

Characteristic		StageI	StageII	StageIII	StageIV	'NA'	Overall
Number of samples		163	70	46	21	7	307
Age (years)		45.9±13.2	49.1±14.2	51.2±13.4	53.3±12.6	58.8±18.8	48.3±13.8
HPV status	Positive	152	63	44	18	7	284
	Negative	11	6	2	3	-	22
	Indeterminate	-	1	-	-	-	1
Smoking history		1.8±1.1	1.7±1.2	1.9±1.1	1.7±1.1	2.7±2.1	1.8±1.2
Pregnancies		3.3±2.1	3.9±3.1	4.1±2.8	3.7±2.4	2.5±2.1	3.6±2.6
Vital status	Alive	135	61	36	8	7	247
	Dead	28	9	10	13	-	60
Histologic Grade	G I/II	84	34	23	11	2	154
	G III/IV	65	27	20	5	4	121

Table 3 (on next page)

Top 10 miRNAs of the linear model.

The log-fold change expression of the miRNA in each stage relative to the controls is given, followed by p-value adjusted for multiple hypothesis testing.

miRNA	Stage I	Stage II	Stage III	Stage IV	adj.P-val
hsa-miR-200c-3p	6.482045	6.481021	6.368438	6.531557	1.96E-20
hsa-miR-141-5p	7.198326	7.176844	6.987161	6.984235	1.96E-20
hsa-miR-141-3p	7.255806	7.393614	7.107695	7.661661	6.69E-20
hsa-miR-200b-5p	6.894887	6.722141	6.676681	6.800084	1.65E-18
hsa-miR-200a-5p	6.6007	6.427489	6.32197	6.630056	3.47E-17
hsa-miR-429	6.457317	6.198339	6.260309	6.738229	1.90E-14
hsa-miR-183-5p	6.65119	6.37214	6.573401	6.790348	1.13E-12
hsa-miR-200a-3p	6.366769	6.32042	6.045745	6.690082	2.50E-12
hsa-miR-21-5p	2.627225	2.74718	2.653042	2.670944	2.50E-12
hsa-miR-182-5p	5.965592	5.618077	5.735565	5.76765	3.67E-12

Table 4(on next page)

Summary of the Cox survival analysis.

It is seen that hsa-miR-625-5p has a significant protective effect on CESC OS, in contrast with hsa-miR-95-3p and hsa-miR-330-3p. The overall multivariate model is very significant with p-value < 0.002. HR denotes hazard rate, and CI confidence interval.

Variables	Analysis	Coefficient	HR (95% CI)	P-value
hsa-miR-95-3p	Univariate	-0.84	0.43 (0.24-0.79)	0.0063
	Multivariate	0.30	1.35 (1.05-1.73)	0.0197
hsa-miR-625-5p	Univariate	1.4	4.2 (1.3-14)	0.0180
	Multivariate	-0.52	0.59 (0.43-0.83)	0.0020
hsa-mir-330-3p	Univariate	-0.68	0.51 (0.28-0.93)	0.0290
	Multivariate	0.35	1.42 (0.98-2.03)	0.0608

HR - hazard rate; CI - confidence interval.